

# MEASURE OF DIVERGENCE AT THE TOP OF TROPICAL CONVECTIVE SYSTEMS FROM WATER VAPOR WINDS

Henri Laurent<sup>(1)</sup> and Meiry S. Sakamoto<sup>(2)</sup>

<sup>(1)</sup> ORSTOM

BP 5045 F-34032 Montpellier, France

<sup>(2)</sup> FUNCEME

Av. Bezerra de Menezes 1900 Fortaleza CE, CEP 60325-002, Brasil

## ABSTRACT

The aim of this work is to study the feasibility of estimating the high level wind divergence associated with tropical convective cloud systems. This approach could be useful to monitor the activity of the deep convection. We explore here the use of full resolution water vapor channel images to estimate the wind vectors in the high troposphere. Numerous and consistent wind vectors can be derived from water vapor image sequences, mainly in the vicinity of high level cloud regions. The water vapor wind vectors are here derived using an algorithm similar to the algorithms used in the operational centers. The main difference consists in adjusting the position of the computation window to center on the brightness gradient maximum, leading to a better tracer selection and a reduction of the number of erroneous vectors passing the automatic quality control. From the drift wind vectors, an interpolation scheme is applied to obtain the wind field on a regular grid. The divergence field is then obtained by finite difference from the interpolated gridded wind field. Special attention has been paid to the interpolation scheme. The results show the importance of interpolating both in space and time, in order to filter out the non persistent fluctuations. Water vapor winds and divergence fields have been computed from METEOSAT images for some case studies of large mesoscale convective systems. Results from a case study corresponding to a very heavy rainfall event in the Sahel are presented here.

## 1. INTRODUCTION

Some of the atmospheric motions can be observed from the geostationary satellites. Infrared (IR) and Visible channels provide good wind observations, but only with clouds. As a consequence, the drift vectors do not present a uniform coverage. The Water Vapor channel (WV) data permit to derive more uniform wind fields by tracking water vapor structures, mainly in the vicinity of high level clouds.

The recent developments in WV tracking techniques, and the various possible applications of the derived fields have been showed by Velden et al. (1997). Considering the potential of this information in high troposphere, Schmetz et al. (1995) made an analysis of monthly mean humidity and divergence fields derived from three different geostationary satellites. Their work showed that this type of data can be used in climatic scale studies.

In the tropics the primary source of energy is the latent heat, which is released mainly in convective cloud systems. Therefore, the knowledge of divergence fields at the top of convective systems is very important to understand the atmospheric circulation. The main objective of this study is to explore the use of WV wind vectors to derive instantaneous divergence fields in tropical regions, and the utility of this information to monitor convective systems.

## 2. METHODOLOGY

### 2.1 Wind derivation

Atmospheric motions are computed from semi hourly images from the Meteosat WV channel (centered at  $6.5 \mu\text{m}$ ) at full resolution ( $5 \times 5 \text{ km}$  at the sub-satellite point). The WV wind extraction procedure is basically described in Laurent (1993). The vector computation is similar to that used in operational centers to derive cloud motion winds from IR or WV images (Schmetz et al., 1993, Velden et al., 1997). There is no distinction between clouds and pure water vapor structures. The processing is entirely automatic, based on a cross correlation scheme where similar patterns are determined in the sequence of three successive WV images.

The algorithm is based on a windowing technique, where a small window, named target window at  $t$  time, searches inside another window placed at time ( $t-30$  minutes) or ( $t+30$  minutes), a similar pattern. The original IR wind derivation utilized by EUMETSAT, considers  $32 \times 32$  pixels as a size of target. Some tests by considering different sizes have been done in a previous work (Sakamoto and Laurent, 1998). These tests suggest that a size of  $16 \times 16$  pixels could be a more suitable size for the target, in order to derive high density wind fields. It should be noted that this suggestion is valid only for Meteosat-5 and later, thanks to a signal to noise reduction that has a large impact on the WV wind production (Laurent, 1993). A  $16 \times 16$  pixel target size has been used in the processing of the results presented here.

Regularly located targets being not always the optimum tracers, some alternative can be considered. Velden et al. (1997) calculate the bi-dimensional gradient for each pixel in the target box and make an identification of the maximum gradient. This gradient undergoes a pixel brightness check to ensure that target are cloudy and contrasted tracers. In our methodology, we calculate the bi-dimensional gradient inside the target window. The location of the target window is then shifted in order to center on the position of the gradient maximum. The wind computation is not performed if the gradient maximum is on the edge of the window, however there is no rejection based on the brightness temperature contrast. This new target window is used to search for the best displacement by cross correlation.

The level assignment is performed by comparison between the brightness temperature of the tracer and a climatologic profile of pressure/temperature. In this study we focus on the high level winds, therefore only tracers with a brightness temperature smaller than  $250 \text{ K}$  are retained, corresponding to a pressure smaller than about  $380 \text{ hPa}$ .

An automatic quality control is performed in order to reject inconsistent drift vectors. Once the best displacement is obtained, the correlation coefficient is calculated between each pair of images. The wind vector is rejected if the coefficient is smaller than 0.5. Vectors with very small velocity ( $V < 3 \text{ ms}^{-1}$ ) are also rejected. Afterwards, the wind vector passes a temporal consistency check, also named symmetry test. This test compares the 2 vectors,  $V_0$  obtained from the pair (t-30 minutes and t) and  $V$  obtained from the pair (t and t+30 minutes). The vector is rejected if :

$$\| V - V_0 \| = 5 + 0.2 * \| V_0 \| \quad (\text{ms}^{-1}) \quad (1)$$

## 2.2 Divergence estimation

Divergence can be computed directly from the drift vector, however the resulting field is very sensitive to the noise of the vectors. It appeared more efficient to interpolate a wind field on a regular mesh, then to derive the divergence by finite difference.

In a preliminary study, Sakamoto and Laurent (1998) used a distance dependent weight, with a parameter adjusted to filter more or less high frequencies in space. They have shown that the approach makes it possible to retrieve divergence fields from WV winds. A comparison with analysis from a global forecast model indicated that unresolved small scale structures could be evidenced by this kind of observations. However the results were not fully satisfactory, because of the large impact of a few erroneous drift vectors on the computed divergence field. Better results can be achieved by exploiting the inherent filtering properties of the Barnes (1964) interpolation scheme. The technique proposed by Doswell (1977) interpolates simultaneously in space and time, imposing a time continuity analogous to that of a subjective analyst. Following Doswell, the value  $\phi_g$  assigned to a gridpoint is the weighted average of the observed values  $\phi_i$ , given by :

$$\phi_g = \frac{\sum_{i=1}^M W_i \phi_i}{\sum_{i=1}^M W_i} \quad (2)$$

where  $W_i$ , the weight of the  $i$  data located at the  $d_i$  distance and at the  $t_i$  time interval of the considered grid point, is defined as :

$$W_i = \exp \{ -(d_i / \delta)^2 - (t_i / \tau)^2 \} \quad (3)$$

the number  $M$  of datum points depends on reasonable limiting values for  $d_i$  and  $t_i$ , and therefore on the choice of the parameters  $\delta$  and  $\tau$ . In this study, the limiting values for  $d_i$  and  $t_i$  are  $2\delta$  and  $2\tau$  respectively. An additional condition is used to ensure that the interpolated value is not too far from observations. The gridpoint value is not considered if :

$$\sum_{i=1}^M W_i < 0.2 \quad (4)$$

The response function in the spectral domain corresponding to (3) is given by :

$$r = \exp ( -(\delta k/2)^2 - (\tau v/2)^2 ) \quad (5)$$

where  $k$  and  $v$  are the wavenumber and the frequency. The response function shows that the interpolation is a low-pass filtering. The parameters  $\delta$  and  $\tau$  defining the radius of influence in space and time can be adjusted to filter high frequencies in space and time respectively.

### 3. CASE STUDY

The results presented here are related to a case study, over West Africa. The date was chosen because a very heavy rainfall event was observed in Niamey, Niger (13.5 N - 2.5 E), where 126 mm were recorded on 1 August 1998 between 3 UTC and 9 UTC. Figure 1 shows the METEOSAT WV image for 1/08/1998 at 3:45 UTC. Red areas correspond to the top of convective clouds in the high troposphere, whereas dark blue are associated with warm and dry air at lower levels. Two very large convective cloud systems are located near 12 N-5 W and 14 N-4 E, and a third one lies at 12 N-18 E.

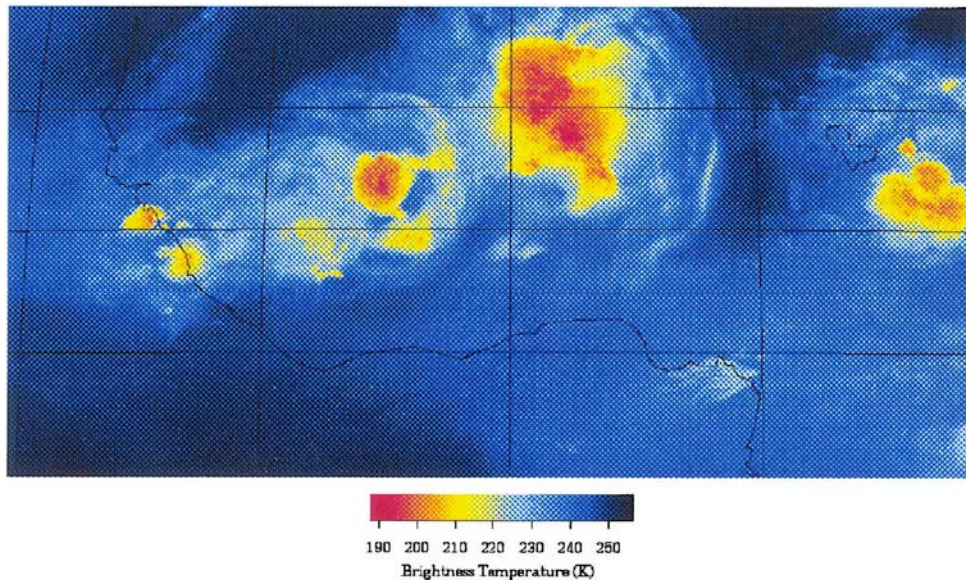


**Figure 1.** METEOSAT Water Vapour channel brightness temperature, 01 August 1998 slot 8 (03:45 UTC).

The WV winds have been derived from a series of METEOSAT WV images from 31 July 12h to 1 August 18h. Figure 2 shows four successive WV wind vectors at the time of the beginning of the rainfall event over the Niamey region. There is a good vector density over and on the edges of the convective cloud shields. Despite of a very simple quality control, only a very few erroneous vectors have been retained (e. g.,  $40 \text{ ms}^{-1}$  NW wind vector at 12 N-12.5W at 04 UTC). The general flow is E or NE, however some wind vectors differ in a small region centered on 7 N-7 E. This is presumably due to the tracking of lower level motions, as in this region the brightness temperature is close to the 250 K threshold.

Figure 3 shows the interpolated wind field obtained on a grid size of 10 latitude x 10 longitude and the corresponding divergence. The  $\delta$  and  $\tau$  parameters are here equal to  $2.5^\circ$  and 1 hour respectively. The smoothing effect evidences the upper part of the Hadley circulation, i. e. divergence at the top of the ITCZ. There are also important convergence areas located between and southward of the main convective systems.

Figure 4 shows the result obtained with a smaller space smoothing effect ( $b = 10$ ). Small scale structures are observed. Two intense divergence areas are located over the two main convective systems, with intensity reaching  $10^{-4} \text{ s}^{-1}$ . They are separated by an intense convergence area ( $-5 \cdot 10^{-5} \text{ s}^{-1}$ ). These structures are persistent during the time sequence shown, between 03 and 06:30



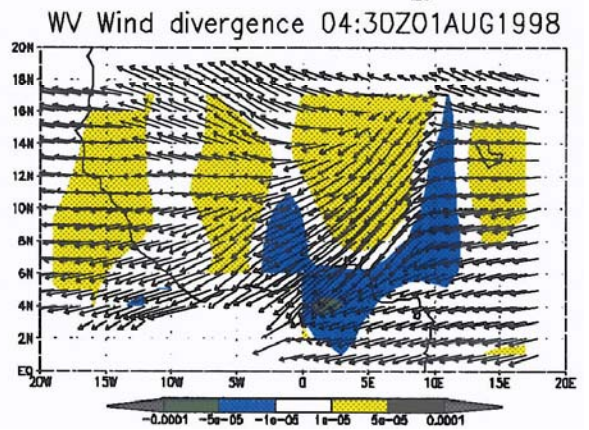
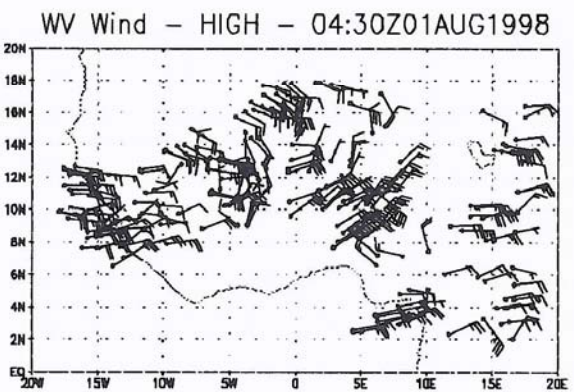
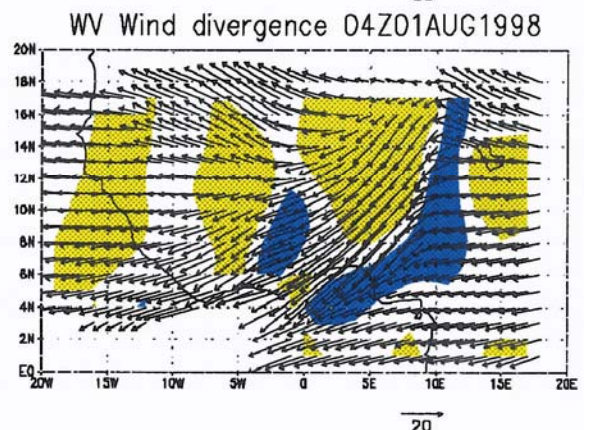
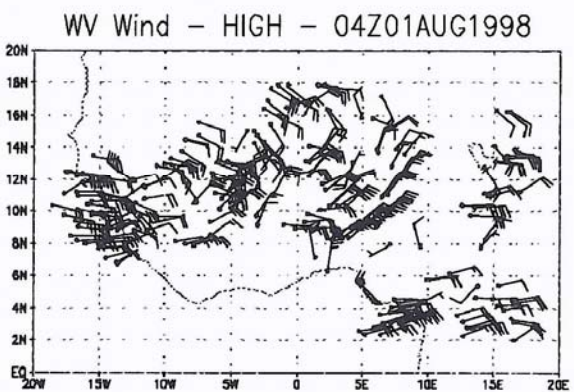
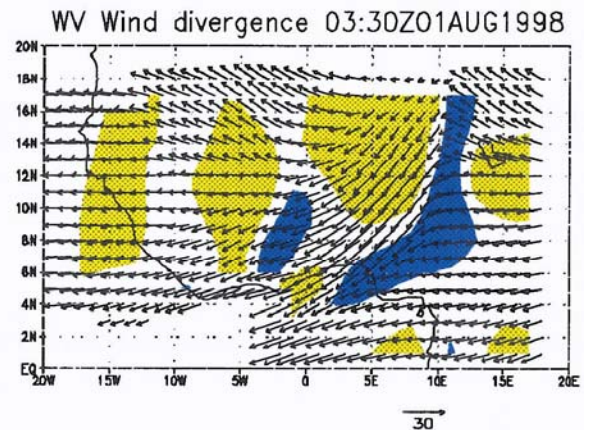
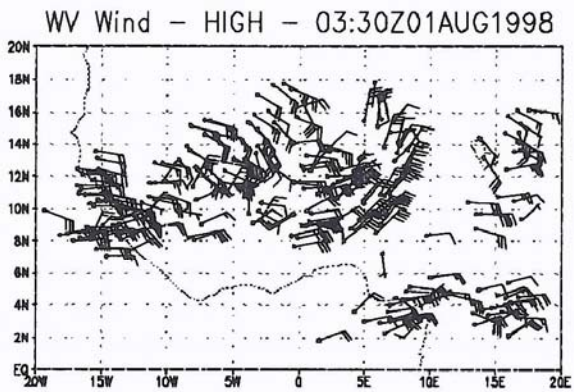
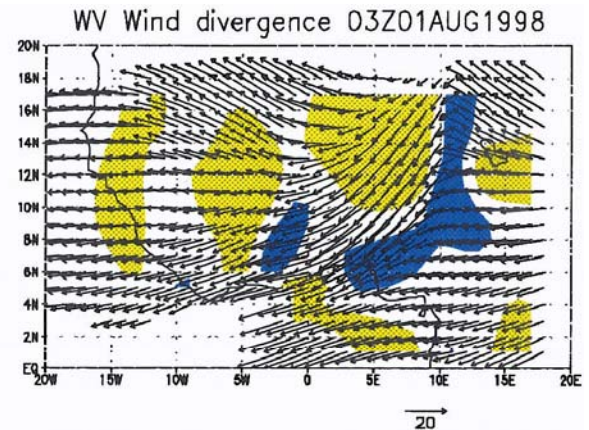
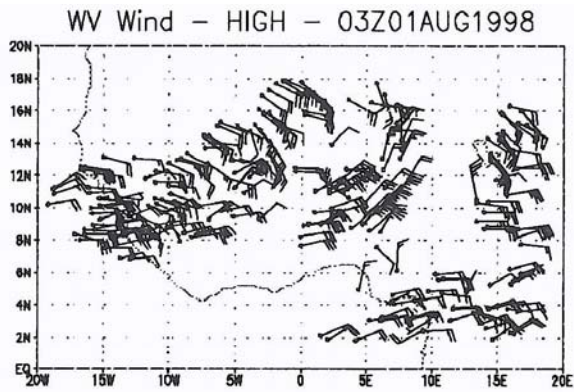


**Figure 2.** High level ( $T < 250\text{K}$ ) WV wind vectors derived from successive Meteosat images, 1 August 1998, between 03 UTC and 04:30 UTC.

**Figure 3.** Interpolated WV wind ( $\text{ms}^{-1}$ ) and divergence ( $\text{s}^{-1}$ ) fields corresponding to Fig. 2. Interpolation parameters:  $\tau = 1 \text{ h}$ ,  $\delta = 2.5^\circ$ .



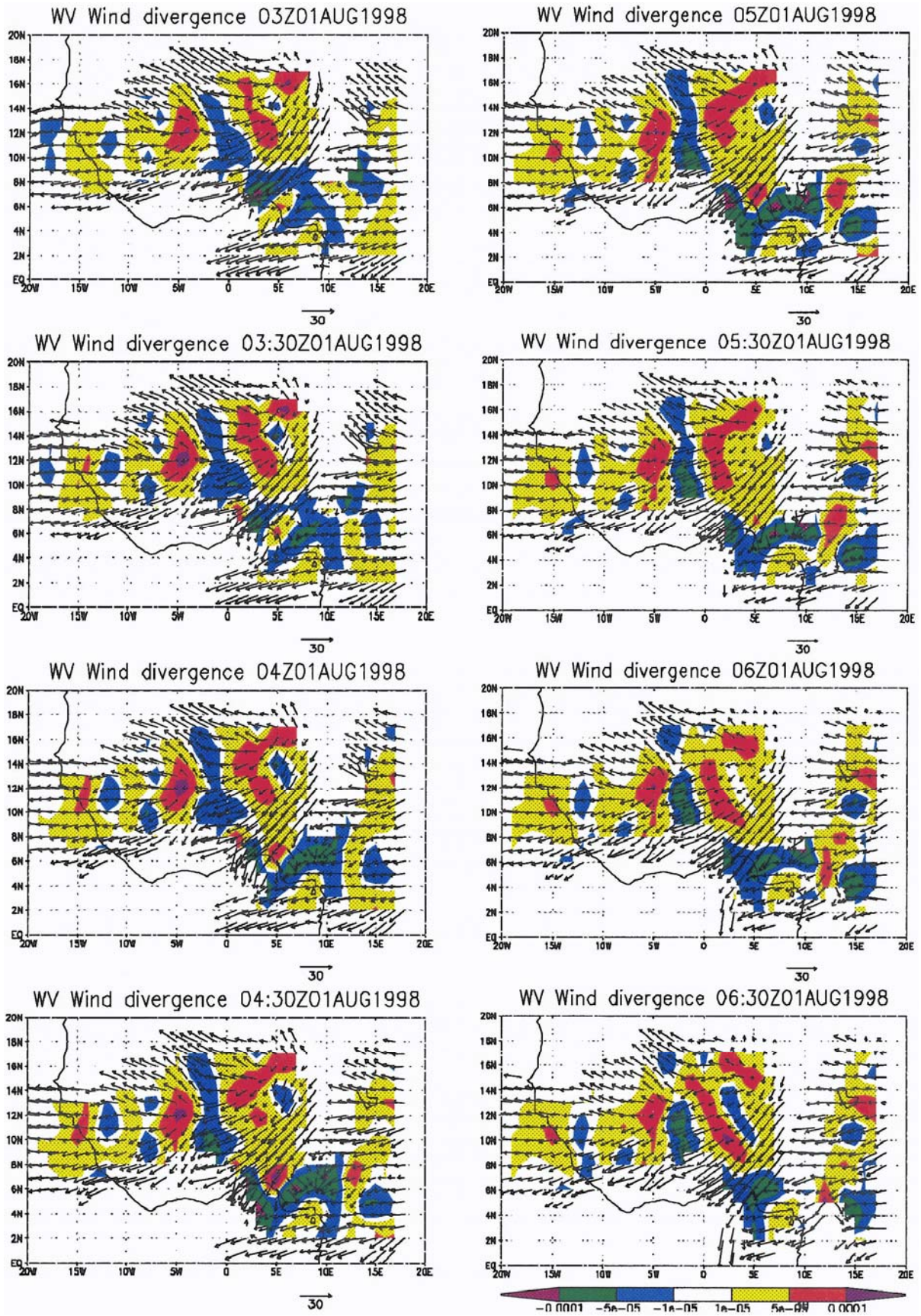


**Figure 4.** Interpolated WV wind ( $\text{ms}^{-1}$ ) and divergence ( $\text{s}^{-1}$ ) fields between 03 UTC and 06:30 UTC. Interpolation parameters :  $\tau = 1 \text{ h}$ ,  $\delta = 1^\circ$ .

UTC. This persistence is not only due to the interpolation applied, firstly because the radius of influence is of one hour, secondly because the structures propagate westward with the cloud systems. The convergence axis visible on Fig. 2 at 11 E between 8 N and 18 N is no more visible due to the lack of gridpoint value at this resolution. The large convergence area near 6 N-5 E is mainly explained by the confluence of two axes of the Tropical Easterly Jet, as can be better seen in Fig. 3. However, part of the variations in this region could be due to a mixing of different levels, as already mentioned.

#### 4. CONCLUSION

The WV winds provide numerous and consistent vectors over large area in the vicinity of high level clouds. However estimation of wind divergence from observations is difficult because of the sensitivity of this quantity. This study shows that the use of an appropriate interpolation scheme, filtering both in space and time, can help to retrieve divergence fields from WV wind vectors.

A major difficulty is that erroneous vectors remain after the quality control step. It is quite encouraging that with the very simple automatic quality control used in this study, only very few erroneous vectors were retained. This is partly attributed to the use of a target position adjustment, based on the brightness gradient calculation. The interpolation both in space and time is powerful to filter non persistent features.

The results from the case study presented here and from a few other case studies suggest that divergence deduced from the WV wind vectors could provide a valuable source of information for the study and for the monitoring of the main convective cloud systems.

#### 5. REFERENCES

- Barnes, S.L., 1964: A technique for maximizing details in numerical weather map analysis. *J. Appl. Meteor.*, 3, 396-409.
- Doswell, C.A., 1977: Obtaining meteorologically significant surface divergence fields through the filtering property of objective analysis. *Mon. Wea. Rev.*, 105, 885-892.
- Laurent, H., 1993: Wind extraction from Meteosat water vapor channel image data. *J. Appl. Meteor.*, 32, 1124-1133.
- Sakamoto M. and H. Laurent, 1998: Measure of divergence at the top of tropical convective systems using wind fields derived from water vapour images. 9th Conference on Satellite Meteorology and Oceanography, Paris, France, 25-29 May 1998. AMS Publ., 356-359.
- Schmetz, J, K. Holmlund, J. Hoffman, B. Strauss, B. Mason, V. Gaertner, A. Koch and L. Van de Berg, 1993: Operational cloud-motion winds from Meteosat infrared images. *J. Appl. Meteor.*, 32, 1206-1225.
- Schmetz, J., W.P.Menzel, C.Velden, X. Wu, L. van de Berg, S. Nieman, C. Hayden, K. Holmlund and C.Geijo, 1995: Monthly mean large-scale analyses of upper-tropospheric humidity and wind field divergence derived from three geostationary satellites. *Bull. Amer. Meteor. Soc.*, 76, 1578-1584.
- Velden, C.S., C.M. Hayden, S.J. Nieman, W.P. Menzel, S. Wanzong and J.S. Goerss, 1997: Upper-tropospheric winds derived from geostationary satellite water vapor observations. *Bull. Amer. Meteor. Soc.*, 78, 173-208.